Prev. Nutr. Food Sci. 2026;31(3):pnf.2026.002
https://doi.org/10.3746/pnf.2026.002
ISSN 2287-8602

Evaluation of the Anti-Inflammatory and Antioxidant Properties of *Mangifera indica* var. *teloor* Extract

Yun Ji Park[1], Rusea Go[2], Mohd. Nazre Salleh[3], Jin Hyub Paik[4], Sang Jin Jo[4], and Sung Keun Jung[1,5]

[1]School of Advanced Bioconvergence and [5]Research Institute of Tailored Food Technology, Kyungpook National University, Daegu 41566, Korea
[2]Department of Biology, Faculty of Science and [3]Faculty of Forestry, Universiti Putra Malaysia, Serdang 43400, Malaysia
[4]International Biological Material Research Center, Korea Research Institute Bioscience and Biotechnology, Daejeon 34141, Korea

ABSTRACT: The genus *Mangifera* belongs to the family Anacardiaceae; *Mangifera indica* (mango) is the best-known species. However, our understanding of the anti-inflammatory effects of *M. indica* var. *teloor* extract (MIE) remains limited. Therefore, this study evaluated the anti-inflammatory and antioxidant activities of *teloor* extracts in murine macrophage RAW 264.7 cells. The MIE significantly suppressed lipopolysaccharide (LPS)-induced nitric oxide (NO) production and inducible NO synthase (*iNOS*) expression, in a dose-dependent manner without causing cytotoxicity. Moreover, MIE inhibited LPS-induced p65 phosphorylation. Cytosol and nucleus fractionation, and Western blots showed that the MIEs suppressed LPS-induced cytosol-nucleus translocation of p65. Furthermore, MIE attenuated LPS-induced abnormal reactive oxygen species production and expression of genes encoding pro-inflammatory cytokines, including interleukin-6 (*IL-6*) and tumor necrosis factor-α (*TNF-α*). These findings suggest that MIE can serve as a functional food ingredient that modulates the NF-kappa B signaling pathway to exert anti-inflammatory and antioxidant activities.

Keywords: antioxidants, biological products, functional food, inflammation, NF-kappa B

INTRODUCTION

The primary function of inflammation is to eliminate harmful stimuli, such as pathogens, or damaged cells and initiate the repair of injured tissues. In contrast, when acute inflammation fails to resolve properly and becomes chronic, it promotes the onset of various chronic inflammatory diseases, including chronic obstructive pulmonary disease and inflammatory bowel disease (Kim and Lee, 2024). These conditions play a prominent role in global mortality, as more than 50% of deaths may be associated with inflammation-driven diseases (Noren Hooten et al., 2023). Therefore, appropriate regulation of these processes and attenuation of excessive inflammation are crucial strategies for preventing disease progression and maintaining physiological homeostasis.

Intracellular signaling pathways regulate the production of inflammatory mediators during immune responses. Among them, the NF-kappa B (NF-κB) pathway is a well-characterized pro-inflammatory cascade activated by pro-inflammatory signals, Toll-like receptors, and lymphocyte receptors (Barnabei et al., 2021). NF-κB exists as a heterodimer composed of p65 and p50, which, in its inactive state, is retained within the cytoplasm (Jang et al., 2024). Upon lipopolysaccharide (LPS) stimulation, the NF-κB complex is released, allowing p65 to translocate into the nucleus and binds to promoter regions of inflammation-related genes, including inducible nitric oxide synthase (*iNOS*) (Magnani et al., 2000), to regulate their transcription. Thus, the NF-κB signaling pathway plays a central role in regulating inflammation and modulating immune responses, thereby representing a major therapeutic target.

Reactive oxygen species (ROS) are highly active molecules involved in essential cellular processes, including autophagy, immune responses, and receptor-mediated signaling (Martinvalet and Walch, 2021). Nitric oxide (NO) functions as a key signaling molecule and participates in various physiological responses, including inflammation and immune regulation (Coleman, 2001). However, excessive ROS and NO production induce oxidative stress, exaggerated inflammatory responses, and the expression of inflammation-related mediators, such as *iNOS* (Mittal et al., 2014). Pro-inflammatory cytokines are rapidly in-

Received 5 January 2026; Revised 3 March 2026; Accepted 4 March 2026; Published online 10 June 2026
Correspondence to Sung Keun Jung, E-mail: skjung@knu.ac.kr

duced by stimuli such as LPS (Page et al., 2022). Tumor necrosis factor-α (*TNF-α*) is a potent pro-inflammatory mediator that plays an essential role in immune regulation during inflammation; it induces severe cytotoxicity, leading to tumor necrosis following immune activation (Zelová and Hošek, 2013). Interleukin-6 (*IL-6*) is a critical mediator of immune responses crucial for host defense; however, excessive or persistent *IL-6* expression promotes the progression of various inflammatory diseases and cancers (Tanaka et al., 2016).

Nonsteroidal anti-inflammatory drugs, corticosteroids, and disease-modifying antirheumatic drugs are commonly used to treat inflammatory disorders. Nevertheless, these conventional therapies exhibit several limitations, including adverse effects, organ toxicity, and drug resistance (Narayanan, 2025). Consequently, identifying safe, naturally derived anti-inflammatory agents has become imperative. *Mangifera indica* var. *teloor*, a variant of mango native to Malaysia, is one such candidate; however, elucidation of its anti-inflammatory and antioxidant properties remains limited, warranting further investigation.

Therefore, this study aimed to evaluate the anti-inflammatory and antioxidant activities of *M. indica* var. *teloor* extract (MIE) in LPS-stimulated RAW 264.7 murine macrophages. Specifically, we assessed the ability of MIE to suppress *iNOS* expression, NO production, oxidative stress, NF-κB-associated transcriptional activity, and inflammatory cytokine production, to determine its potential as a functional health-promoting bioactive ingredient.

MATERIALS AND METHODS

Materials and reagents

Dulbecco's modified Eagle's medium (DMEM), 1% antibiotic (penicillin/streptomycin solution), and 10% fetal bovine serum (FBS) were purchased from Thermo Fisher Scientific. LPS derived from *Escherichia coli* O111:B4 (LPS25) and thiazolyl blue tetrazolium bromide were bought from Sigma-Aldrich. For Western blots, the primary antibodies against *iNOS*, cyclooxygenase-2 (*COX*-2), phospho-p65 (Ser536), p65, α/β-tubulin, and PCNA were obtained from Cell Signaling Technology, whereas anti-β-actin was purchased from Santa Cruz Biotech. Antibodies were diluted 1:1,000 in 1x Tris-buffered saline (TBS) containing 0.1% Tween® 20 Detergent (TBS-T) according to the protocols provided. Horseradish peroxidase-conjugated secondary antibodies, Pierce Goat Anti-Mouse IgG (H+L), and Pierce Goat Anti-Rabbit IgG (H+L), were purchased from Thermo Fisher Scientific. NE-PER™ Nuclear and Cytoplasmic Extraction Reagents were purchased from Thermo Fisher Scientific.

Sample preparation and extraction

The MIE (FBM287-075) used in this study was collected from Serdang, Selangor, Malaysia, and provided by the Korea Research Institute of Bioscience and Biotechnology (KRIBB), Daejeon, South Korea. The plant samples were collected and identified by Prof. Rusea Go from the Department of Biology, Universiti Putra Malaysia, Seri Kembangan, Malaysia. A voucher specimen "MK319" was deposited in the KRIBB herbarium. The leaves and stems of *M. indica* var. *teloor* were collected, ground, shade-dried, and powdered. Then, 70 g of the material was mixed with 1 L of 99.9% methanol (HPLC grade). Subsequently, the samples were extracted at room temperature (RT) with an ultrasonic extractor (SDN-900H, SD-Ultrasonic Co., Ltd.) for 30 cycles: 40 kHz, 1,500 W, 15 min ultrasonication, 120 min standing/cycle. The extract was filtered (Qualitative Filter No. 100, Hyundai Micro Co., Ltd.) and vacuum-dried. Thus, 70 g of plant material yielded 2 g of extract, with a final yield of 2.86%. This extract was dissolved in dimethyl sulfoxide (DMSO, Sigma-Aldrich) to obtain a concentration of 100 mg/mL.

Cell culture

The murine macrophage cell line RAW 264.7 was purchased from the Korean Cell Line Research Foundation, Seoul, South Korea. The cells were cultured in DMEM or high-glucose medium supplemented with 10% FBS and 1% antibiotics at 37°C in an incubator with 5% CO_2.

Cytotoxicity assessment

RAW 264.7 cells were seeded into 96-well plates at 2×10^5 cells/mL, 100 μL per well, and incubated under 5% CO_2 at 37°C for 24 h. After draining the medium, the cells were treated with MIE at 25, 50, and 100 μg/mL−100 μL per well−and incubated for another 24 h. Subsequently, 10 μL of MTT was added to each well, and the plates were incubated for 2 h. Finally, 80 μL of the supernatant from each well was collected, 100 μL of DMSO was added, the plate was wrapped with aluminum foil (to avoid light exposure), and shaken at 100 rpm for 30 min. The absorbance at 595 nm of each well was then measured using a microplate reader (Molecular Devices) to evaluate cytotoxicity.

Quantification of NO

RAW 264.7 cells were seeded into 96-well plates at 3×10^5 cells/mL, 200 μL per well, and incubated under 5% CO_2 at 37°C for 24 h. After draining the medium, the cells were pre-treated with MIE at 25, 50, and 100 μg/mL−200 μL per well−for 1 h. Subsequently, 25, 50, or 100 μg/mL MIE dissolved in a medium containing 1 μg/mL LPS was added−200 μL per well−and incubated for 24 h. Finally, 100 μL of each cell culture supernatant was transferred to a fresh 96-well plate. Sodium nitrite

(Sigma-Aldrich Co.) served as a standard. It was diluted to a concentration range of 0–100 μM and added at 100 μL per well. Equal volumes of Griess A [0.2% N-(1-naphthyl)-ethylenediamine dihydrochloride] and Griess B (1% sulfanilamide in 5% phosphoric acid) were then added to all wells. The plate was shaken for 15 min, and the absorbance at 550 nm was measured using a microplate reader. The absorbance values of different concentrations of sodium nitrite were used to generate a standard curve for NO.

Western blots

RAW 264.7 cells were seeded into Petri dishes at 2×10^5 cells/mL and incubated under 5% CO_2 at 37°C for 24 h. Then, the dishes were placed on ice, the medium was removed, and the cells were washed twice with phosphate-buffered saline (PBS). Cell lysis buffer (Cell Signaling Technologies) was added, and the cell lysates were collected in 1.5 mL tubes. The tubes were kept on ice and vortexed 3 times for >30 min. They were then centrifuged at 13,572 *g* and 4°C for 15 min. The supernatant was collected, and its protein concentration was determined employing a DC Protein Assay kit (Bio-Rad Laboratories, Inc.). The cell lysates were diluted with sterile distilled water and 5X SDS sample buffer and loaded onto a 10% acrylamide gel. Proteins were separated via electrophoresis and then transferred to a polyvinylidene difluoride membrane (Immobilon-P transfer membrane, Millipore) at 4°C for 1 h. To prevent non-specific binding, the membrane was blocked with TBS-T containing 5% skim milk at RT for 1 h and then incubated with primary antibodies at 4°C overnight. Then, the membrane was washed 3 times with TBS-T and incubated with the appropriate secondary antibody at RT for 1 h. Finally, the membrane was rewashed 3 times with TBS-T and treated with the Lumi Plus reagent. Proteins were visualized and quantified with GeneGnome XRQ NPC system (Syngene). Cytosolic and nuclear fractions were isolated using NE-PER™ Nuclear and Cytoplasmic Extraction Reagents according to the manufacturer's instructions. The extracted proteins were quantified using a DC Protein Assay kit and subjected to Western blot analysis.

Immunofluorescence assays

RAW 264.7 cells were seeded into an 8-well chamber (ibidi) at 1×10^5 cells/mL, 200 μL per well, and incubated under 5% CO_2 at 37°C for 24 h. After removing the medium, the cells were pre-treated with MIE at 25, 50, or 100 μg/mL−200 μL per well−for 1 h. Subsequently, they were treated with MIE at 25, 50, or 100 μg/mL dissolved in a medium containing 1 μg/mL LPS−200 μL per well−for 24 h. Next, 4% formaldehyde was added to the plates at 200 μL/well and incubated for 15 min. After fixation, the cells were permeabilized with cold 100% methanol. The samples were blocked at RT for 1 h and then incubated overnight with the primary anti-p65 antibody at 4°C. Afterward, the samples were incubated with the secondary antibody: Alexa Fluor® 488-conjugated goat anti-rabbit IgG H&L (Abcam) for 1 h, followed by nuclear staining with DAPI (VECTASHIELD, Vector Laboratories). The translocation of p65 was visualized using fluorescence microscopy (Leica Microsystems).

Evaluation of ROS scavenging activity

RAW 264.7 cells were seeded into 96-well plates at 3×10^5 cells/mL, 100 μL per well, and incubated under 5% CO_2 at 37°C for 24 h. After removing the medium, the cells were pre-treated with MIE at 25, 50, or 100 μg/mL−100 μL per well−for 1 h. Subsequently, they were treated with MIE at 25, 50, or 100 μg/mL dissolved in a medium containing 1 μg/mL LPS−200 μL per well−and incubated for 24 h. Next, each well was washed twice with 200 μL of PBS and 200 μL of serum-free medium containing 2',7'-dichlorofluorescein diacetate (DCF-DA; 20 mM) and incubated for 30 min. After staining, the wells were washed twice with 200 μL PBS. The intensity of ROS-induced fluorescence was measured at 485–535 nm with a microplate fluorometer (Molecular Devices). ROS generation was visualized using fluorescence microscopy and analyzed by employing the LAS X microscope software (Leica Microsystems).

Quantitative reverse transcription polymerase chain reaction (qRT-PCR)

RAW 264.7 cells were seeded into Petri dishes at 2×10^5 cells/mL and incubated under 5% CO_2 at 37°C for 24 h. The cells were then pre-treated with MIE at 25, 50, or 100 μg/mL for 1 h, and stimulated with 1 μg/mL LPS for 24 h. Next, the Petri dishes were placed on ice, the medium was removed, and the cells were washed twice with PBS. Total RNA was extracted using RNA isolation buffer (Takara Bio), and cDNA was synthesized using ReverTra Ace™ qPCR RT Master Mix (TOYOBO) and DEPC-treated water. qRT-PCR was performed on the CFX Connect real-time PCR detection system (Bio-Rad Laboratories) to amplify specific genes. The expression levels of pro-inflammatory cytokine-encoding genes were normalized to those of the housekeeping gene *GAPDH* using the ΔΔCq method. The primer nucleotide sequences for *TNF-α* and *IL-6* are presented in Table 1.

Statistical analysis

All results are presented as the mean±standard deviation. The data were analyzed using GraphPad Prism 9 software. Differences between the control and MIE-treated groups were analyzed using a *t*-test and one-way

Table 1. Primer sequences of the target-gene-specific primers

Target gene	Sense strand (5′→3′)	Antisense strand (3′→5′)
Mouse *GAPDH*	TCA ACG GCA CAG TCA AGG	ACT CCA CGA CAT ACT CAG C
Mouse *TNF-α*	TGG AAC TGG CAG AAG AGG CAC T	AGA GGC TGA GAC ATA GGC ACC G
Mouse *IL-6*	TGG GAC TGA TGC TGG TGA CAA C	AGC CTC CGA CTT GTG AAG TGG T

TNF-α, tumor necrosis factor-α; *IL-6*, interleukin-6.

analysis of variance. Statistical significance was determined at $P<0.05$ compared with the control group.

RESULTS AND DISCUSSION

Effects of MIE on LPS-induced NO production and viability in RAW 264.7 cells

NO is a critical signaling molecule that regulates vascular function, immune responses, and the activities of immune and inflammatory cells under normal physiological conditions (Yin et al., 2019). However, excessive NO production can trigger abnormal inflammatory responses and contribute to the pathogenesis of chronic inflammatory diseases, including tissue damage (Wang et al., 2015). Thus, this study investigated the inhibitory influence of MIE on LPS-induced overproduction of NO in RAW 264.7 cells. Compared to the control group, treatment with 1 μg/mL LPS significantly increased NO biosynthesis; in contrast, pre-treatment with MIE at concentrations of 25, 50, and 100 μg/mL markedly suppressed NO production in a dose-dependent manner (Fig. 1A). Notably, NO production was inhibited by 75.7% with 100 μg/mL treatment group. Jo et al. (2025) have previously reported that extracts of *Urceola polymorpha* (Pierre ex Spire) D.J. Middleton & Livsh. inhibited NO biosynthesis by 74.6%, and that of *Pyrolae herba* extract suppressed production by 42.9% (Lee et al., 2007). While these comparisons provide a reference, such pronounced effects of MIE are likely attributable to its remarkable interference with LPS-induced inflammatory signaling pathways that regulate *iNOS* expression and excessive NO production, rather than to a generalized cell-level suppression (Li et al., 2002). From this mechanistic perspective, the concentration-dependent reduction in NO production by MIE appears to reflect the stepwise inhibition of LPS-induced *iNOS* expression and its upstream components of inflammatory signaling cascades. Therefore, these findings suggest that MIE remarkably attenuates LPS-induced inflammation by regulating NO biosynthesis. Furthermore, MTT assay results showed that MIE was not cytotoxic at the test concentrations, indicating that it can safely inhibit inflammatory responses in RAW 264.7 cells without affecting viability (Fig. 1B).

Effects of MIE on LPS-induced *iNOS* and *COX-2* expression in RAW 264.7 cells

NO, synthesized by *iNOS*, is a vital inflammatory mediator *iNOS* (Choi et al., 2009). Meanwhile, excessive NO levels are closely linked to the pathogenesis of inflammatory diseases. Pre-treatment with MIE significantly reduced LPS-induced NO production in a dose-dependent manner. We further evaluated the effects of MIE on the expression of *iNOS* and *COX-2* using Western blots. Pre-treatment effectively suppressed *iNOS* expression in a dose-dependent manner but not that of *COX-2* (Fig. 2). This selective inhibition *iNOS* may be attributed to variations in the regulatory mechanisms governing these two inflammation-associated genes. Although *iNOS* and

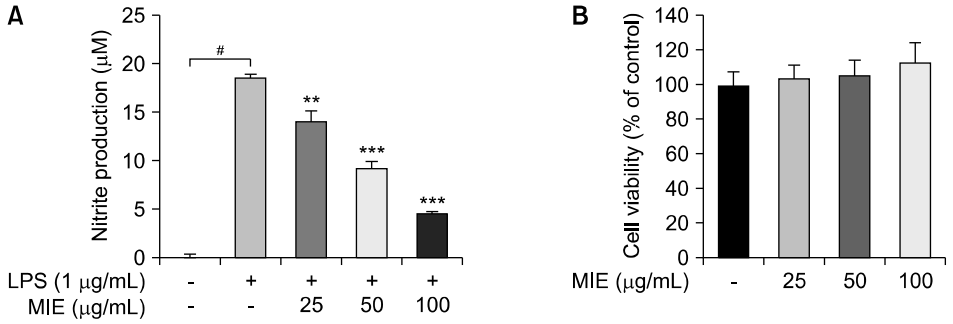

Fig. 1. Effect of *Mangifera indica* var. *teloor* extract (MIE) on lipopolysaccharide (LPS)-induced nitric oxide (NO) production and viability in RAW 264.7 cells. (A) MIE inhibited LPS-induced NO production in a dose-dependent manner. (B) MIE at any concentration did not affect cell viability. The cells were treated with MIE at 25, 50, or 100 μg/mL for 24 h. $^{\#}P<0.05$ indicates a statistically significant difference between the control and LPS-treated groups, while $^{**}P<0.01$ and $^{***}P<0.001$ represent statistically significant variations between the LPS+MIE-treated and LPS-exposed groups. Data are presented as the mean±standard deviation of three independent experiments.

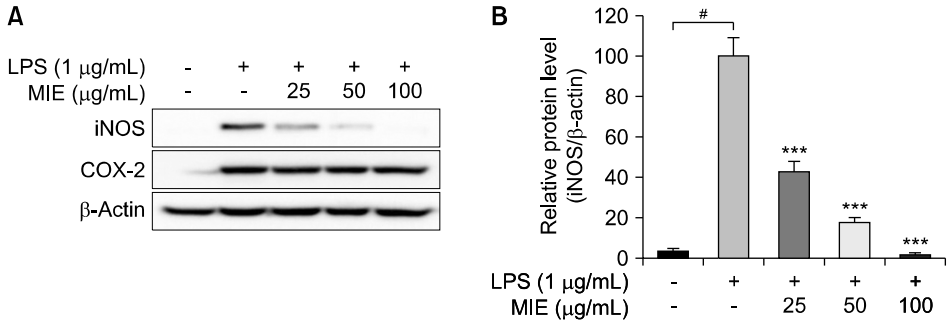

Fig. 2. Effect of *Mangifera indica* var. *teloor* extract (MIE) on lipopolysaccharide (LPS)-induced inducible NO synthase (*iNOS*) and cyclooxygenase-2 (*COX-2*) expression in RAW 264.7 cells. (A) MIE inhibited the LPS-induced enhancement in the expression of *iNOS* in a dose-dependent manner but did not affect *COX-2*. The cells were treated with MIE at 25, 50, or 100 μg/mL for 24 h. (B) Quantitative analysis of the suppressive effects of MIE on LPS-induced *iNOS* protein expression. The protein contents of *iNOS*, COX-2, and β-actin were determined by Western blots. $^{\#}P<0.05$ indicates a statistically significant difference between the control and LPS-treated groups, while $^{***}P<0.001$ represents statistically significant variations between LPS+MIE-treated and LPS-exposed groups. Data are presented as the mean±standard deviation of three independent experiments.

COX-2 are downstream targets of NF-κB signaling, *iNOS* expression is more strongly dependent on NF-κB activation. In contrast, that of *COX-2* is regulated by multiple transcription factors, including CRE and AP-1, which may render it less sensitive to a partial suppression of NF-κB signaling (Lee et al., 2009). Post-transcriptional regulatory mechanisms may also contribute, as *iNOS* mRNA is less stable and more susceptible to degradation than *COX-2* transcripts (Lisi et al., 2011). Therefore, the preferential downregulation of *iNOS* by MIE suggests that it selectively interferes with inflammatory pathways governing excessive NO biosynthesis rather than broadly suppressing all pro-inflammatory enzymes. Collectively, these findings indicate that MIE exerts anti-inflammatory impacts in RAW 264.7 cells mainly by inhibiting *iNOS*-mediated NO production rather than affecting *COX-2* protein expression.

Effects of MIE on LPS-induced NF-κB signaling in RAW 264.7 cells

Activation of the NF-κB pathway is commonly evaluated based on the phosphorylation status of p65, the major transcriptionally active subunit of NF-κB. It provides a reliable indicator of NF-κB activation without the need to assess additional pathway components (Hochrainer et al., 2013); thus, we employed this method to evaluate whether MIE affects NF-κB pathway activation. The results revealed that MIE remarkably inhibited LPS-induced p65 phosphorylation in RAW 264.7 cells (Fig. 3), suggesting that MIE may suppress NF-κB activation by inhibiting p65 phosphorylation, thereby reducing *iNOS* expression and inflammatory responses.

Effects of MIE on LPS-induced nuclear translocation of p65 in RAW 264.7 cells

The cytoplasm-nucleus translocation of p65 is a key indicator of NF-κB activation (Florio et al., 2022). *Paeonia lactiflora* extracts exerted an anti-inflammatory influence by inhibiting translocation of p65 from the cytoplasm to the nucleus (Kim et al., 2021). Therefore, we evaluated the impacts of MIE on LPS-induced p65 translocation in RAW 264.7 cells. Subsequent immunofluorescence anal-

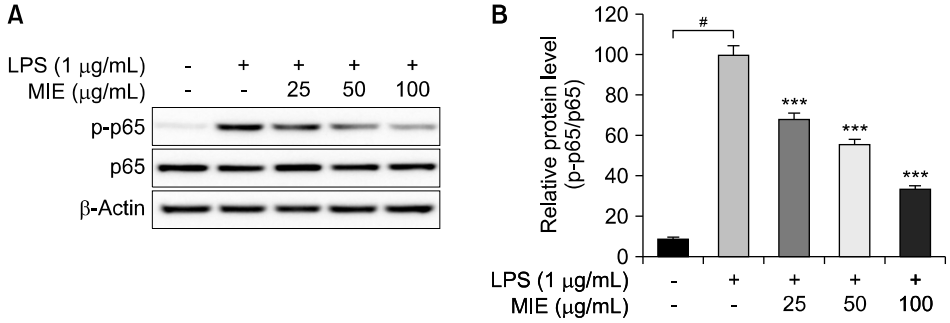

Fig. 3. Effect of *Mangifera indica* var. *teloor* extract (MIE) on lipopolysaccharide (LPS)-induced activation of the NF-κB signaling pathway in RAW 264.7 cells. (A and B) MIE inhibited LPS-induced phosphorylation of p65 in a dose-dependent manner. The cells were treated with MIE at 25, 50, or 100 μg/mL for 30 min. The p65 and β-actin were quantified by Western blots. $^{\#}P<0.05$ indicates a statistically significant difference between the control and LPS-treated groups, while $^{***}P<0.001$ represents statistically significant variations between LPS+MIE-treated and LPS-exposed groups. Data are presented as the mean±standard deviation of three independent experiments.

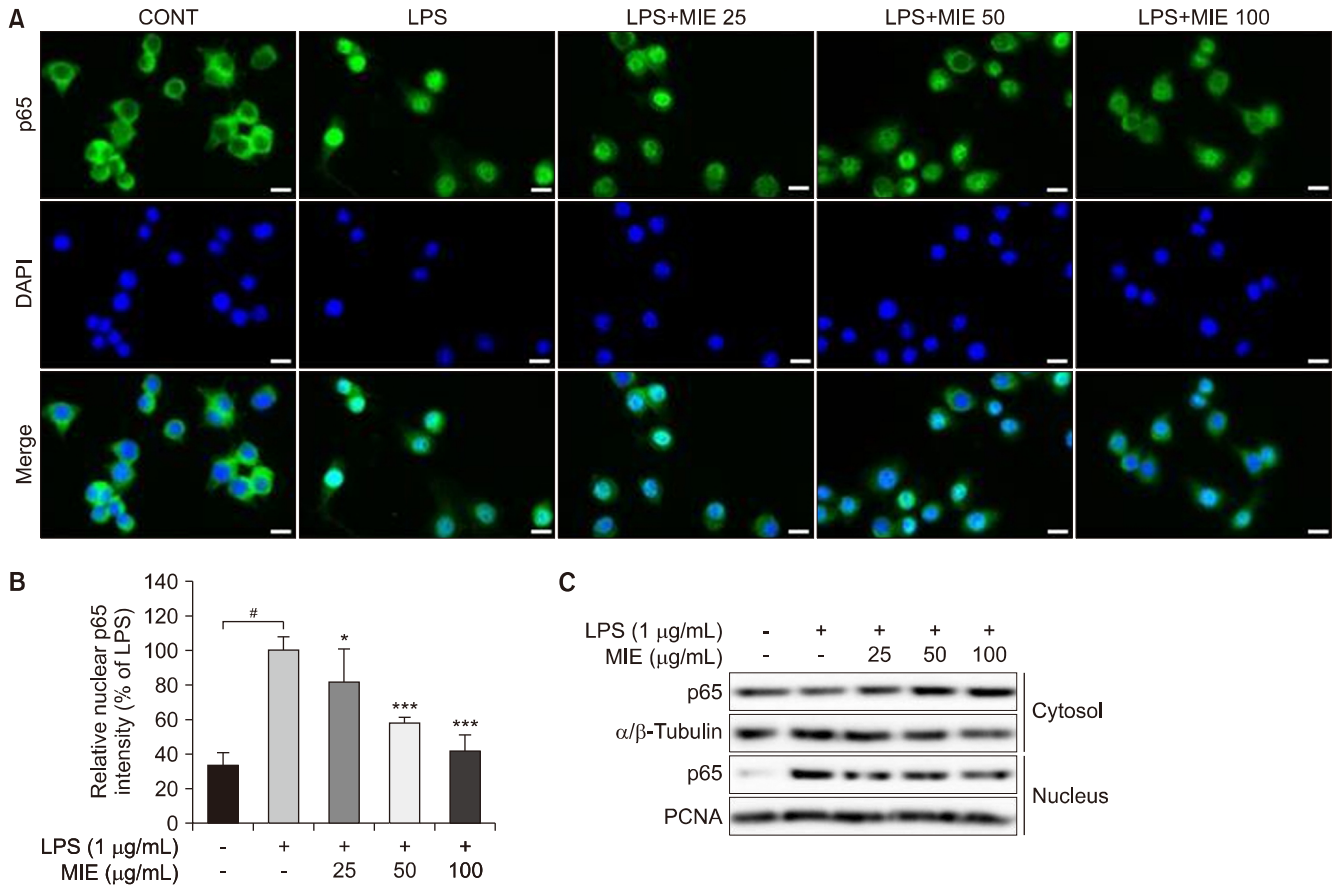

Fig. 4. Effect of *Mangifera indica* var. *teloor* extract (MIE) on lipopolysaccharide (LPS)-induced translocation of p65 from the cytoplasm to the nucleus in RAW 264.7 cells. (A, B, and C) MIE suppressed this translocation in a dose-dependent manner. Cells were treated with MIE at 25, 50, or 100 μg/mL for 24 h. Fluorescence intensities of five randomly selected cells per group were quantified. $^{\#}P<0.05$ indicates a statistically significant variation between the control and LPS-treated groups, while $^{*}P<0.05$ and $^{***}P<0.001$ represent statistically significant differences between the LPS+MIE-treated group and the LPS-exposed group. Data are presented as the mean±standard deviation of three independent experiments. Scale bar=20 μm.

ysis revealed that LPS significantly enhanced p65 translocation; in contrast, MIE markedly attenuated this translocation in a concentration-dependent manner (Fig. 4). These findings indicate that MIE suppresses NF-κB activation by inhibiting the nuclear translocation of p65, thereby contributing to the anti-inflammatory effect.

Effects of MIE on LPS-induced alterations in inflammatory cytokines in RAW 264.7 cells

Cytokines coordinate immune cell activity and regulate inflammation to combat infection. However, excessive cytokine production can lead to hyperinflammation, thereby serving as a critical marker of dysregulation in the inflammatory response (Fajgenbaum and June, 2020). Consequently, we investigated the regulatory effects of MIE on LPS-induced inflammatory responses in RAW 264.7 cells by analyzing the transcription of inflammatory cytokine-encoding genes using qRT-PCR. These results showed that LPS stimulation markedly increased *TNF-α* and *IL-6* mRNA levels compared with the control group. However, MIE pre-treatment markedly suppressed LPS-induced upregulation of *TNF-α* in a dose-dependent manner (Fig. 5A). LPS-induced expression of *IL-6* was suppressed by MIE pre-treatment, although the reduction was statistically insignificant (Fig. 5B). These findings indicate that MIE possesses anti-inflammatory activity by downregulating critical inflammatory cytokines, such as *TNF-α*, while reducing *IL-6* expression.

Effects of MIE on LPS-induced ROS production in RAW 264.7 cells

Elevated ROS levels contribute to the initiation and progression of inflammation, linking oxidative stress to various inflammatory diseases (Mittal et al., 2014). Since the two are closely interconnected, we evaluated the impacts of MIE on LPS-induced ROS production in RAW 264.7 cells using DCF-DA. LPS significantly enhanced ROS generation, which was markedly attenuated by 100 μg/mL MIE, reducing ROS synthesis by 69.5% (Fig. 6). Fluorescence microscopy observations supported these results (Fig. 6B). *Zanthoxylum myriacanthum* Wall. ex Hook. f. extracts inhibited LPS-induced ROS production by ~51.4% (Seong et al., 2024). These findings suggest that MIE can attenuate LPS-induced ROS syn-

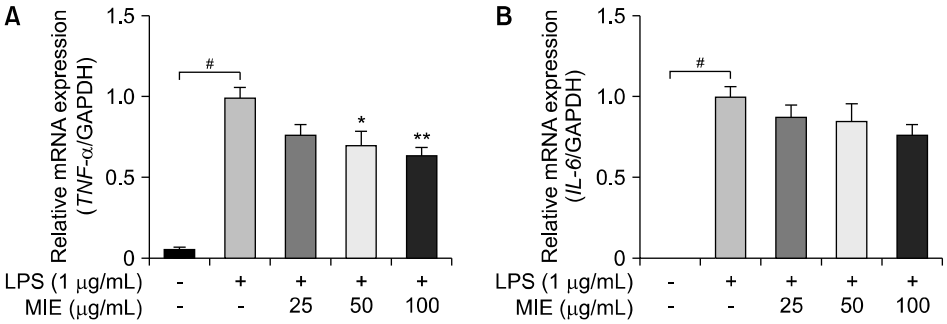

Fig. 5. Effect of *Mangifera indica* var. *teloor* extract (MIE) on lipopolysaccharide (LPS)-induced alterations in inflammatory cytokine levels in RAW 264.7 cells. (A and B) MIE suppressed the LPS-induced upregulation of tumor necrosis factor-α (*TNF-α*) and interleukin-6 (*IL-6*). Cells were treated with MIE at 25, 50, or 100 μg/mL for 24 h. $^{\#}P<0.05$ indicates a statistically significant variation between the control and LPS-treated groups, while $^{*}P<0.05$ and $^{**}P<0.01$ represent statistically significant differences between LPS+MIE-treated and LPS-exposed groups. Data are presented as the mean±standard deviation of three independent experiments.

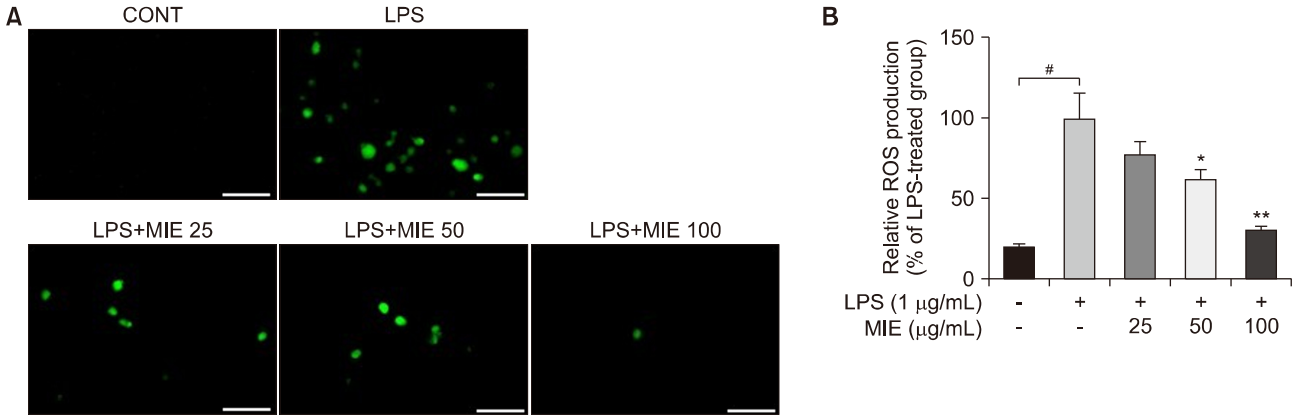

Fig. 6. Effect of *Mangifera indica* var. *teloor* extract (MIE) on lipopolysaccharide (LPS)-induced reactive oxygen species (ROS) production in RAW 264.7 cells. (A and B) MIE suppressed LPS-induced ROS generation in a dose-dependent manner. Cells were treated with MIE at 25, 50, or 100 μg/mL for 24 h. $^{\#}P<0.05$ represents a statistically significant difference between the control and LPS-treated groups, while $^{*}P<0.05$ and $^{**}P<0.01$ indicate statistically significant variations between the LPS+MIE-treated and LPS-exposed groups. Data are presented as the mean±standard deviation of three independent experiments. Scale bar=50 μm.

thesis in RAW 264.7 cells, demonstrating its potential as an antioxidant with free-radical-scavenging activity.

We identified MIE as one of the most potent natural anti-inflammatory materials by screening the plants obtained from the KRIBB for NO inhibition. MIE significantly inhibited LPS-induced NO production and *iNOS* expression at non-cytotoxic concentrations. Moreover, MIE suppressed the phosphorylation of p65 and its subsequent cytoplasm-nucleus translocation. MIE also reduced LPS-induced ROS production and the mRNA levels of pro-inflammatory cytokines markedly. These findings suggest that MIE may serve as an anti-inflammatory agent by regulating LPS-induced *iNOS* and NO production, as well as NF-κB signaling pathway activation.

FUNDING

This research was supported by the KRIBB Initiative Program of the Republic of Korea and the National Research Foundation of Korea (NRF-2022R1A2C1010923).

AUTHOR DISCLOSURE STATEMENT

The authors declare no conflict of interest.

AUTHOR CONTRIBUTIONS

Concept and design: SKJ. Analysis and interpretation: YJP. Data collection: YJP, RG, MNS, JHP, SJJ. Writing the article: YJP. Critical revision of the article: SKJ. Final approval of the article: All authors. Statistical analysis: YJP. Obtained funding: SKJ. Overall responsibility: SKJ.

REFERENCES

Barnabei L, Laplantine E, Mbongo W, Rieux-Laucat F, Weil R.

NF-κB: At the borders of autoimmunity and inflammation. Front Immunol. 2021. 12:716469. https://doi.org/10.3389/fimmu.2021.716469

Choi Y, Lee MK, Lim SY, Sung SH, Kim YC. Inhibition of inducible NO synthase, cyclooxygenase-2 and interleukin-1β by torilin is mediated by mitogen-activated protein kinases in microglial BV2 cells. Br J Pharmacol. 2009. 156:933-940. https://doi.org/10.1111/j.1476-5381.2009.00022.x

Coleman JW. Nitric oxide in immunity and inflammation. Int Immunopharmacol. 2001. 1:1397-1406. https://doi.org/10.1016/s1567-5769(01)00086-8

Fajgenbaum DC, June CH. Cytokine storm. N Engl J Med. 2020. 383:2255-2273. https://doi.org/10.1056/NEJMra2026131

Hochrainer K, Racchumi G, Anrather J. Site-specific phosphorylation of the p65 protein subunit mediates selective gene expression by differential NF-κB and RNA polymerase II promoter recruitment. J Biol Chem. 2013. 288:285-293. https://doi.org/10.1074/jbc.M112.385625

Jang S, Kim S, Kim SJ, Kim JY, Gu DH, So BR, et al. Innate immune-enhancing effect of *Pinus densiflora* pollen extract via NF-κB pathway activation. J Microbiol Biotechnol. 2024. 34:644-653. https://doi.org/10.4014/jmb.2309.09026

Jo HJ, Bach TT, Eum SM, Jung SK. Anti-inflammatory and antioxidant effects of *Urceola polymorpha* (Pierre ex Spire) D.J.Middleton & Livsh. Extract via regulation of the NF-κB pathway. J Korean Soc Food Sci Nutr. 2025. 54:157-163. https://doi.org/10.3746/jkfn.2025.54.2.157

Kim ME, Lee JS. Molecular foundations of inflammatory diseases: Insights into inflammation and inflammasomes. Curr Issues Mol Biol. 2024. 46:469-484. https://doi.org/10.3390/cimb46010030

Kim MJ, Kang HH, Seo YJ, Kim KM, Kim YJ, Jung SK. *Paeonia lactiflora* root extract and its components reduce biomarkers of early atherosclerosis via anti-inflammatory and antioxidant effects in vitro and in vivo. Antioxidants. 2021. 10:1507. https://doi.org/10.3390/antiox10101507

Lee JA, Song HY, Ju SM, Lee SJ, Kwon HJ, Eum WS, et al. Differential regulation of inducible nitric oxide synthase and cyclooxygenase-2 expression by superoxide dismutase in lipopolysaccharide stimulated RAW 264.7 cells. Exp Mol Med. 2009. 41:629-637. https://doi.org/10.3858/emm.2009.41.9.069

Lee MH, Lee JM, Jun SH, Lee SH, Kim NW, Lee JH, et al. The anti-inflammatory effects of *Pyrolae herba* extract through the inhibition of the expression of inducible nitric oxide synthase (iNOS) and NO production. J Ethnopharmacol. 2007. 112:49-54. https://doi.org/10.1016/j.jep.2007.01.036

Li YH, Yan ZQ, Brauner A, Tullus K. Activation of macrophage nuclear factor-κB and induction of inducible nitric oxide synthase by LPS. Respir Res. 2002. 3:23. https://doi.org/10.1186/rr173

Lisi L, Navarra P, Feinstein DL, Dello Russo C. The mTOR kinase inhibitor rapamycin decreases iNOS mRNA stability in astrocytes. J Neuroinflammation. 2011. 8:1. https://doi.org/10.1186/1742-2094-8-1

Magnani M, Crinelli R, Bianchi M, Antonelli A. The ubiquitin-dependent proteolytic system and other potential targets for the modulation of nuclear factor-kB (NF-kB). Curr Drug Targets. 2000. 1:387-399. https://doi.org/10.2174/1389450003349056

Martinvalet D, Walch M. Editorial: The role of reactive oxygen species in protective immunity. Front Immunol. 2021. 12:832946. https://doi.org/10.3389/fimmu.2021.832946

Mittal M, Siddiqui MR, Tran K, Reddy SP, Malik AB. Reactive oxygen species in inflammation and tissue injury. Antioxid Redox Signal. 2014. 20:1126-1167. https://doi.org/10.1089/ars.2012.5149

Narayanan KB. Enzyme-based anti-inflammatory therapeutics for inflammatory diseases. Pharmaceutics. 2025. 17:606. https://doi.org/10.3390/pharmaceutics17050606

Noren Hooten N, Mode NA, Allotey S, Ezike N, Zonderman AB, Evans MK. Inflammatory proteins are associated with mortality in a middle-aged diverse cohort. Clin Transl Med. 2023. 13:e1412. https://doi.org/10.1002/ctm2.1412

Page MJ, Kell DB, Pretorius E. The role of lipopolysaccharide-induced cell signalling in chronic inflammation. Chronic Stress. 2022. 6:24705470221076390. https://doi.org/10.1177/24705470221076390

Seong HK, Bach TT, Eum SM, Kim MJ, Son JE, Jung SK. Anti-inflammatory and anti-oxidant effects of *Zanthoxylum myriacanthum* Wall. ex Hook. f. extract in RAW 264.7 macrophages. J Korean Soc Food Sci Nutr. 2024. 53:661-668. https://doi.org/10.3746/jkfn.2024.53.7.661

Tanaka T, Narazaki M, Masuda K, Kishimoto T. Regulation of IL-6 in immunity and diseases. Adv Exp Med Biol. 2016. 941:79-88. https://doi.org/10.1007/978-94-024-0921-5_4

Wang CN, Duan GL, Liu YJ, Yu Q, Tang XL, Zhao W, et al. Overproduction of nitric oxide by endothelial cells and macrophages contributes to mitochondrial oxidative stress in adrenocortical cells and adrenal insufficiency during endotoxemia. Free Radic Biol Med. 2015. 83:31-40. https://doi.org/10.1016/j.freeradbiomed.2015.02.024

Yin M, Zhang Y, Li H. Advances in research on immunoregulation of macrophages by plant polysaccharides. Front Immunol. 2019. 10:145. https://doi.org/10.3389/fimmu.2019.00145

Zelová H, Hošek J. TNF-α signalling and inflammation: interactions between old acquaintances. Inflamm Res. 2013. 62:641-651. https://doi.org/10.1007/s00011-013-0633-0